A Decision Tree Approach for Identifying the Optimum Window Size for Extracting Texture Features from TerraSAR-X Data

John Richard OTUKEI, Thomas BLASCHKE and Michael COLLINS

Abstract

Synthetic Aperture Radar (SAR) texture is an important derived variable for improving land cover classification accuracy from SAR data. However, a number of factors affect the amount and quality of texture information obtained from radar data and these include: the window size, data type, the size of grey level quantisation, displacement and the look direction. The main aim of this study was to determine the optimum window size for the extraction of texture features from TerraSAR-X (TSX) data and to study the effect of different window sizes on the classification accuracy of the selected land cover types. A new approach based on Decision Trees (DTs) was explored to determine the optimum window size for SAR texture analysis and the results compared with those obtained using Transformed Divergence (TD) and Jeffries Matusita (JM) statistical distance measures. In all the three approaches, a window size of 11 by 11 was found to be the most appropriate. Generally, the classification accuracy increased with the size of texture window. However, in all the three approaches, there was little increase in classification accuracy beyond a window size of 11 by 11.

1 Introduction

Synthetic Aperture Radar (SAR) data provide complimentary information for land cover mapping, especially in tropical regions often affected by cloud cover. This is because of the ability of radar signal to penetrate through cloud cover (ROSENQVIST, SHIMADA et al. 2000, STANKIEWICZ 2002). Several studies have been carried out to explore the potential of SAR for land cover classification (CHAND & BADARINAHTH 2007, JOOST & HOEKMAN 1999, KUPLICH 2006, RAUSTE 2005, ROSENQVIST,SHIMADA et al. 2000, STANKIEWICZ 2002, SAATCHI & RIGNOT 1997, WASKE & BRAUN 2009, SHUPE & MARSH 2004, PIERCE, BERGEN et al. 1998, DELL' ACQUA, GAMBA et al. 2009). A major challenge of data acquired by SAR systems is the limited number of polarisations, which directly affects the amount of information extracted from radar images. The SAR image texture has been used in some studies to improve on the identification and classification of land cover types from SAR data with limited polarisations (SOARES, RENNO et al. 1997, HEROLD, HAACK et al. 2004, HAACK & BECHDOL 2000, RYHERD & WOODCOCK 1996, SIMARD, SAATCHI et al. 2000). While it is acknowledged that SAR texture plays a significant role in improving the land cover classification from SAR images, the analysis of SAR texture is in itself complex.

First, defining texture is almost as difficult as measuring it (MATHER 2004). Perhaps the simplest definition is that texture is the frequency of tonal change in an image (LILLESAND, KIEFER et al. 2008).The difficulty in defining the term texture has led to a large number of

Jekel, T., Car, A., Strobl, J. & Griesebner, G. (Eds.) (2012): GI_Forum 2012: Geovizualisation, Society and Learning. © Herbert Wichmann Verlag, VDE VERLAG GMBH, Berlin/Offenbach. ISBN 978-3-87907-521-8.

possible texture measures that can be computed for remote sensing data analysis. Generally, SAR texture can be categorised as: SAR specific textures (SARTEX), textures based on grey level co-occurrence matrices (GLCM) and textures based on image histogram (HISTEX). Secondly, there are a number of factors to be considered prior to texture derivation. This includes the selection of appropriate window size, data type, the grey level quantisation, displacement and the look direction. The effect of the aforementioned parameters on the performance of texture features have been studied and details can be found in the work of CLAUSI (2002). However, there is less available information on the methodology for selecting the most appropriate window size for texture derivation. The general observation is that a large window size provides more accurate classification results. Nevertheless, such a general statement may not be helpful in selecting the appropriate window size for texture derivation. As a result, existing studies suggest window sizes of 13×13 (HAACK & BECHDOL 2000), 15×15, 31×31, 61×61 (BLOM 1982), and 13×13, 21×21, 29×29 (HEROLD, HAACK et al. 2004). This presents diversity in the possible window sizes, making it difficult to define the most appropriate window size for a given task. Additionally, while such window sizes have been recommended based on specific studies and other SAR data, none were based on TerraSAR-X (TSX) data analysis. Accordingly, this study set out to determine the most appropriate window for derivation of TSX texture using Decision Trees (DTs). Furthermore, there is no existing study that has shown the use of DTs for determining the optimum window size for texture derivation using any SAR data.

2 Study Area

The study area is the Bwindi Impenetrable National Park (BINP) located in South Western Uganda and covers an area of approximately 331km^2. It is located within $0^0$53'S-$1^0$08'S and $29^0$35'E-$29^0$50' E. The BINP lies at the edge of the great Western Rift Valley and is part of the highest blocks of the Kigezi and Rukiga Highlands. It lies east of the Democratic Republic of Congo (DRC) border, about 29 km by road North West of Kabale, 20 km north of Kisoro, and 40km south east of Lake Edward. The landscape is rugged and characterized by deep narrow valleys with steep sided hills. The area has a wide altitude range, from 1160m at the tip of the northern sector to 2607m at the Rwamunyonyi hill on the south-eastern edge of the Park (UNESCO 2009). The vegetation in the park is characterised as an *afromontane* forest which is considered to be the rarest forest vegetation type on the continent and surrounded by small subsistence farmlands.

3 Materials and Methods

3.1 Data

Two scenes of Enhanced Ellipsoidal Corrected (EEC) TSX data, with a spatial resolution of 2.75m were used for the analysis. The two scenes dated December 4, 2009 and December 15, 2009 comprised of a Horizontal-Horizontal (HH) and Vertical-Vertical (VV) polarization. The TSX space mission is known to be the first German project to be implemented under private-public partnership (PPP) between the German aerospace centre

(DLR) and the EADS Astrium GMbH. The TerraSAR-X instrument is an active phased array X-band system with a centre frequency of 9.65GHz (NONAKA, ISHIZUKA et al. 2008).

3.2 Pre-processing

Pre-processing operations involved mosaicking of the two original TSX scenes as well as extraction of SAR texture features. For this study, nine textures based on GLCM listed in Table 1 were selected for assessing the most appropriate window. The textures were derived using the HH polarisation of the TSX data. Overall, 16 window sizes were examined: 3×3, 5×5, 7×7, 9×9, 11×11, 13×13, 15×15, 17×17, 19×19, 21×21, 23×23, 25×25, 27×27, 29×29, 31×31, 61×61. This range of window sizes was designed to cover all the recommended window sizes from existing studies. In all cases, directional invariant textures were computed using a displacement of 1 and grey level quantisation of 32.

3.3 Analysis of the appropriate window size

Analysis of the appropriate window size was done using the Jeffries Matusita (JM), Transformed Divergence (TD) and Decisions Trees (DTs).

3.3.1 Jeffries Matusita and Transformed Divergence

The JM and TD are statistical distance measures that have been used in remote sensing applications to show not only the separability between any given two signatures computed using any given combination of bands, but also to perform band optimisation (MATHER 2004). The mathematical formulations of JM and TD, according to ERDAS (2009) are as follows:

$$JM_{ij} = \sqrt{2(1 - e^{-\alpha})}$$

Where:

$$\alpha = \frac{1}{8}(\mu_i - \mu_j)^T \left(\frac{C_i + C_j}{2}\right)^{-1} (\mu_i - \mu_j) + \frac{1}{2}\ln\left(\frac{\left|(C_i + C_j)/2\right|}{\sqrt{|C_i| \times |C_j|}}\right)$$

$$TD_{ij} = 2000\left(1 - \exp\left(\frac{-D_{ij}}{8}\right)\right)$$

$$D_{ij} = \frac{1}{2} tr\left((C_i - C_j)(C_i^{-1} - C_j^{-1})\right) + \frac{1}{2} tr\left((C_i^{-1} - C_j^{-1})(\mu_i - \mu_j)(\mu_i - \mu_j)^T\right)$$

The subscripts *i, j* are the signatures of the selected classes, C_i and C_j are the covariance matrices of *i* and *j*, μ_i and μ_j are the mean vectors of *i* and *j*, *ln* is the natural logarithm, *tr* is the trace function and *T* is the matrix transpose. Both the JM and TD have lower and upper

bounds of 0 and 2 respectively, which are multiplied by 1000 in Erdas Imagine software to give a range of 0-2000. In either case, the ranges show how well the classes are separable. The upper bounds indicate very high separability between classes while lower bounds show non-separable classes. Accordingly, the intermediate values show varying degrees of separability.

In order to investigate the appropriate window size for extraction of TSX features using the JM and TD, representative samples of selected land cover classes were delineated. The selected classes were open water (OW), degraded wetland (DW), dense forest (DF) and farmland (F). These classes represented both uniform and heterogeneous classes. All the nine texture features were used as input variables. Pairwise separability was computed using the JM and TD algorithms and the results were used to select the appropriate window size.

Table 1: Textures based on GLCM

Texture	Formula
Homogeneity (HOM)	$\sum_{i,j=0}^{N-1}((p_{i,j})/(1+(i-j)^2))$
Contrast (CON)	$\sum_{i,j=0}^{N-1}((p_{i,j})*(i-j)^2)$
Dissimilarity (DIS)	$\sum_{i,j=0}^{N-1}((p_{i,j})*\mid i-j\mid)$
Mean (M)	$\sum_{i,j}^{N-1}(i*(p_{i,j}))$
Standard Deviation (SD)	$\sqrt{\sum_{i,j=0}^{N-1}P_{i,j}(i-\mu_i)^2}$
Entropy (ENT)	$\sum_{i,j=0}^{N-1}P_{i,j}*(-\ln(P_{i,j}))$
Ang. 2nd. Moment (ASM)	$\sum_{i,j}^{N-1}(p_{i,j})^2$
Correlation (CORR)	$\sum_{i,j=0}^{N-1}\left[\frac{(i-\mu_i)(j-\mu_j)}{\sqrt{(\sigma_i^2)(\sigma_i^2)}}\right]$
Inverse Distance (ID)	$\sum_{i,j=0}^{N-1}((p_{i,j})/(i-j)^2)$

3.3.2 Decision Trees

DTs are non-parametric classification approaches that do not require assumptions about data distribution (OTUKEI & BLASCHKE 2010). They are characterised as data mining tools

which are used in machine learning for solving classification problems and other related tasks (Quinlan, 1993). The structure of DTs comprise one root node, a number of interior nodes and a set of terminal nodes linked using decision stages (OTUKEI & BLASCHKE 2010, TSO & MATHER 2001). Consequently, the construction of DTs follows a multi-stage and sequential approach to problem solving (MAHESH & MATHER 2003). It involves the recursive partitioning of space defined by the training dataset into homogenous subsets on the basis of the data supplied by either one or more features. This results in either univariate or multivariate DTs. In order to assign unknown value to one of the given classes, a decision rule is needed at each node. For univariate DTs, this can be of the form:

$$\sum_{i=1}^{n} a_i x_i \leq c$$

Where: x_i is the measurement vector of n selected features, a_i is the vector of coefficients of linear discriminate functions and c is the threshold value. DTs are an attractive method for analysis of TSX since they are not constrained by normal distribution assumptions required for parametric classifiers. Furthermore, studies have shown that DTs perform better or at least produce results of comparable accuracies to those obtained using traditional classification approaches (OTUKEI & BLASCHKE 2010).

The analysis of window size using DTs was performed by computing the kappa statistic which is one of the parameters used to express land cover classification accuracy. Prior to image classification, data representing each of the selected classes were prepared in a format readable in WEKA (Waikato Environment for Knowledge Analysis) software. A classification was performed using the J48 decision tree classifier, a WEKA implementation of Quilan's C4.5 DT classifier (BOUCKAERT, FRANK et al. 2010, WITTEN & FRANK 2005). At any given window size, the classification kappa index (κ) was noted. In each case, a 10-fold cross validation was adapted and the resulting kappa values were used to assess the appropriate window for texture analysis.

4 Results and Discussion

Figures 1 and 2 show the relationships between texture window size and interclass separabilities derived using the JM and TD algorithms. The resulting curves of separability indices plotted against the window sizes show both an exponential and saturating behaviour. Some existing studies have also reported similar patterns (JENSEN 1996). The maximum separation between OW and other classes was achieved using a window size of 3×3 for both JM and TD approaches. The ease in separating OW and other classes can be attributed to the homogeneity in the OW class resulting in low SAR intensity variance. However, different window sizes were required to attain maximum separation for other class pairs. For the case of TD, a window size of 9×9 was the minimum size required to attain maximum separation for all the class pairs. On the contrary, the JM approach required a window size of 17×17 to attain a maximum separation between DF-DW and DW-F, while DF-F required window size of 31×31.

The observed difference between the separability of DF-F at 17×17 and 31×31 window sizes was only 0.2. This suggests that a window size of 17×17 provides an acceptable

separability for the DF-F class pair. It can be observed that separating DF and F was difficult due to the high heterogeneity in both classes leading to high SAR intensity variance. As a result, large texture windows would be required to attain maximum separability. Figure 3 shows the relationship between the kappa indices derived using the DT approach with the varying window sizes. Similar to the JM and TD, an exponentially increasing curve was observed implying that classification accuracy increased with the texture window size. Absolute kappa indices however, showed that a maximum kappa index was achieved using a window size of 19×19. Window sizes of 11×11 up to 17×17 also provided high kappa indices of 0.9.

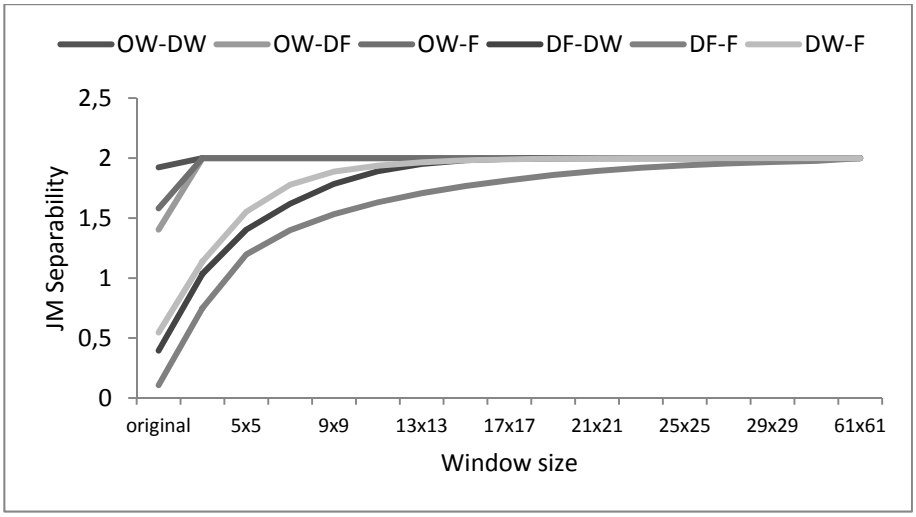

Fig. 1: Window size analysis based on JM distance measure

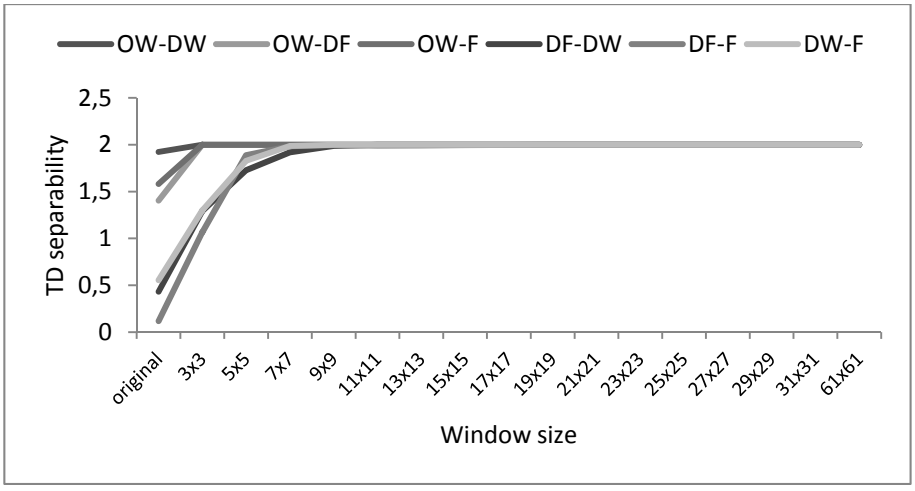

Fig. 2: Window size analysis based on TD distance measure

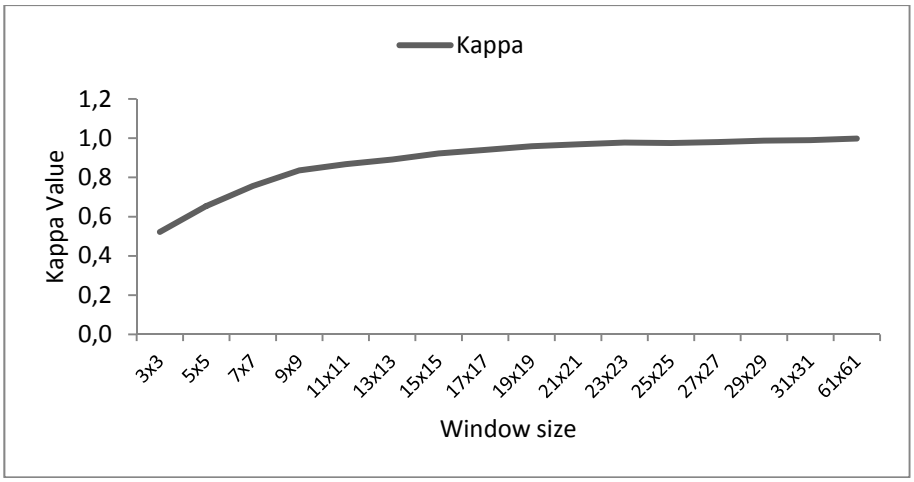

Fig. 3: Window size analysis based on DTs

Overall, with the exception of TD approach, it was not easy to identify a single appropriate window size for separating all classes using the curves shown in Figures 1 and 3. This was due to the exponential nature of the curves. Accordingly, a new concept of rate of change (ROC) was introduced to facilitate visualisation and selection of the appropriate window size. The result of this analysis is shown in Figure 4. A drastic decrease in the ROC was observed up to a window size of 11×11 for JM and TD and 9×9 for the DTs. Beyond these values, no significant difference was noted within each curve. In order to minimise the reduction of information caused by large window sizes as well as to increasing the classification accuracy, a window size of 11×11 was considered appropriate for all the three methods used.

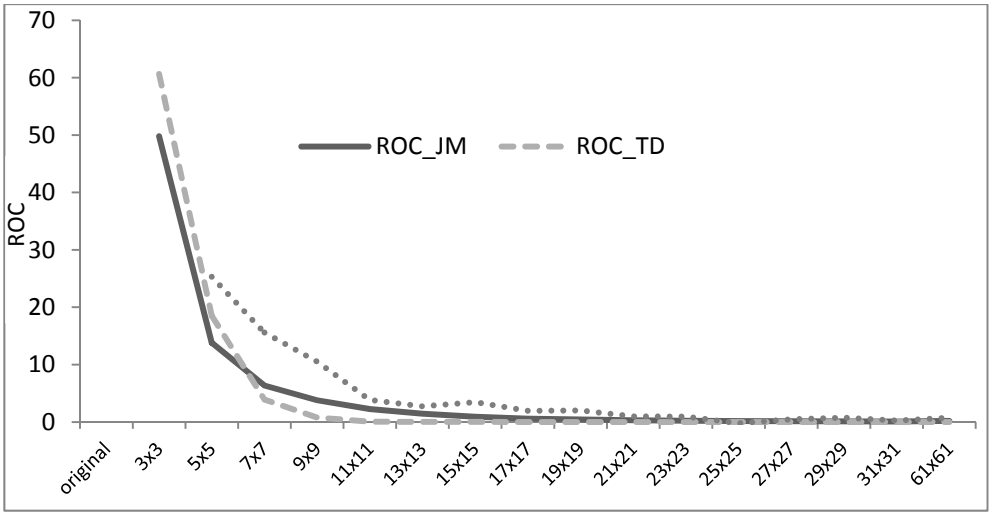

Fig. 4: Relationship between ROC of Kappa, JM, and TD with window size

5 Conclusion

The main aim of this study was to investigate the most appropriate window size for derivation of TSX texture and to investigate the effect of varying window size on classification accuracy of land cover. Based on the results obtained using TD and JM separability measures, as well as those obtained using DTs, it was concluded that a window size of 11×11 s provides the most appropriate for TSX texture extraction. Additionally, the DT approach provides high potential for texture window analysis since it is not affected by parametric assumptions that are difficult to meet using SAR data. Besides, the DTs provide an indication of classification accuracy since the kappa statistics is used instead of interclass separabilities. However, it is important to note that the window size is a function of classes of interest. Large window sizes are required for classes with high TSX intensity variance, while small window sizes are appropriate for classes with low SAR intensity variance.

Acknowledgement

The data was obtained courtesy of UNESCO-DLR open initiative for use of space-borne sensors for monitoring world heritage sites. We would therefore like to thank UNESCO/DLR for providing the TSX data under projected ID LAN0599.

References

BLOM, R. G. (1982), Radar image processing for rock types. IEEE Transactions on Geoscience and Remote Sensing, GE-20, 343-351.

BOUCKAERT, R. R., FRANK, E., HALL, M. et al. (2010), WEKA manual for version 3-7-1. The University of Waikato, Hamilton, New Zealand.

CHAND, T. R. K. & BADARINAHTH, K. V. S. (2007), Analysis of ENVISAT ASAR data for forest parameter retrieval and forest type classification – a case study over deciduous forests of central India. International Journal of Remote Sensing, 28, 4985-4999.

CLAUSI, D. A. (2002), Analysis of co-occurance texture statistics as a function of grey level quantisation Can. J. Remote Sensing, 28, 45-62.

DELL' ACQUA, F., GAMBA, P. & LISINI, G. (2009), Rapid mapping of high resolution SAR scenes. ISPRS Journal of Photogrammerty and Remote Sensing, 64, 482-489.

ERDAS (2009), Erdas field guide, Atlanta, Georgia, Erdas Inc.

HAACK, B. & BECHDOL, M. (2000), Intergrating multisensor data and RADAR texture for land cover mapping. Computers & Geosciences, 26, 411-421.

HEROLD, N. D., HAACK, B. N. & SOLOMON, E. (2004), An evaluation of Radar texture for land use/cover extraction in varied landscapes. International Journal of Applied Earth Observation and GeoInformation, 5.

JENSEN, J. R. (1996), Introductory Digital Image Processing: A Remote Sensing Perspective., Englewood Cliffs, New Jersey, Prentice-Hall.

JOOST, J. V. D. S. & HOEKMAN, D. H. (1999), Potential of airborne radar to support the assessment of land cover in a tropical rain forest environment. Remote Sens. Environ, 68.

KUPLICH, T. M. (2006), Classifying regenerating forest stages in Amazonia using remotely sensed images and a neural network. Forest Ecology and Managment, 234, 1-9.

LILLESAND, T. M., KIEFER, R. W. & CHIPMAN, J. W. (2008), Remote Sensing and Image Interpretation, 6th Edition, Madison, John Wiley & Sons, Inc.

MAHESH, P. & MATHER, P. M. (2003), An assessment of the effectiveness of decision tree methods for land cover classification. Remote Sensing of the Environment, 86, 554-565.

MATHER, P. M. (2004), Computer processing of remotely sensed images: An Introduction, 3rd Edition, West Sussez, England, John Willey and Sons.

NONAKA, T., ISHIZUKA, Y., YAMANE, N. et al. (2008), Evaluation of the geometric accuracy of TerraSAR-X International archives of Photogrammetry and Remote sensing, XXXVII.

OTUKEI, J. R. & BLASCHKE, T. (2010), Land cover mapping using decision trees, support vector machines and maximum classification algorithms. International Journal of Applied Earth Observation and GeoInformation, 12S, S27-S31.

PIERCE, L. E., BERGEN, K. M., DOBSON, M. E. et al. (1998), Multitemporal land cover classification using SIR-C/X-SAR imagery. Remote Sens. Environ, 64, 20-33.

QUINLAN, J. R. (1993), Programs for Machine Learning, Francisco, USA, Morgan Kaufman.

RAUSTE, Y. (2005), Multi-temporal JERS SAR data in boreal forest biomass mapping. Remote Sensing of Environment, 97, 263-275.

ROSENQVIST, Ä., SHIMADA, M., CHAPMAN, B. et al. (2000), The global rain forest mapping project – a review. Int. J. Remote Sensing, 21, 1375-1387.

RYHERD, S. & WOODCOCK, C. (1996), Combining spectral and texture data in the segmentation of remotely sensed images. Photogrammetric Engineering and Remote Sensing, 62, 181-194.

SAATCHI, S. S. & RIGNOT, E. (1997), Classification of Boreal Forest cover using SAR Images. Remote Sens. Environ, 60, 270-281.

SHUPE, S. M. & MARSH, S. E. (2004), Cover and density based vegetation classifications of the Sonoran Desert using Landsat TM and ERS-1 SAR imagery. Remote Sensing of Environment, 93, 131-149.

SIMARD, M., SAATCHI, S. S. & DE GRANDI, G. (2000), The use of decision tree and multiscale texture for classification of JERS-1 SAR data over tropical Forest. IEEE Transactions on Geoscience and Remote Sensing, 38.

SOARES, J. V., RENNO, C. D., FORMAGGIO, A. R. et al. (1997), An investigation of the selection of texture features for crop discrimination using SAR imagery. Remote Sensing of Environment, 59, 234-247.

STANKIEWICZ, K. (2002), The use of microwave SAR images for forest decline monitoring in mountaineous area. Adv. Space Res., 29, 67-72.

TSO, B. & MATHER, P. M. (2001), Classification methods for remote sensed images. London, Taylor & Francis.

UNESCO (2009), Bwindi Impenetrable National Park. http://whc.unesco.org/en/list/682 (accessed June 23, 2009).

WASKE, B. & BRAUN, M. (2009), Classifier ensembles for land cover mapping using multitemporal SAR imagery. ISPRS Journal of photogrammerty and remote sensing, 64, 450-457.

WITTEN, I. H. & FRANK, E. (2005), Data mining: Practical machine tools and techniques, San Francisco, USA, Morgan, Kaufman.